UCSF
UC San Francisco Previously Published Works

Title

Activation of Extracellular Signal-Regulated Kinase but Not of p38 Mitogen-Activated Protein Kinase Pathways in Lymphocytes Requires Allosteric Activation of SOS

Permalink

Journal

ISSN

Authors

Jun, Jesse E
Yang, Ming
Chen, Hang
et al.

Publication Date

DOI

Activation of Extracellular Signal-Regulated Kinase but Not of p38 Mitogen-Activated Protein Kinase Pathways in Lymphocytes Requires Allosteric Activation of SOS

Jesse E. Jun,[a] Ming Yang,[b] Hang Chen,[c] Arup K. Chakraborty,[b,c,d,e,f] Jeroen P. Roose[a]

Department of Anatomy, University of California, San Francisco, San Francisco, California, USA[a]; Departments of Chemical Engineering,[b] Chemistry,[c] Physics,[d] and Biological Engineering[e] and Institute of Medical Engineering & Science,[f] Massachusetts Institute of Technology, Cambridge, Massachusetts, USA

Thymocytes convert graded T cell receptor (TCR) signals into positive selection or deletion, and activation of extracellular signal-related kinase (ERK), p38, and Jun N-terminal protein kinase (JNK) mitogen-activated protein kinases (MAPKs) has been postulated to play a discriminatory role. Two families of Ras guanine nucleotide exchange factors (RasGEFs), SOS and RasGRP, activate Ras and the downstream RAF-MEK-ERK pathway. The pathways leading to lymphocyte p38 and JNK activation are less well defined. We previously described how RasGRP alone induces analog Ras-ERK activation while SOS and RasGRP cooperate to establish bimodal ERK activation. Here we employed computational modeling and biochemical experiments with model cell lines and thymocytes to show that TCR-induced ERK activation grows exponentially in thymocytes and that a W729E allosteric pocket mutant, SOS1, can only reconstitute analog ERK signaling. In agreement with RasGRP allosterically priming SOS, exponential ERK activation is severely decreased by pharmacological or genetic perturbation of the phospholipase Cγ (PLCγ)-diacylglycerol-RasGRP1 pathway. In contrast, p38 activation is not sharply thresholded and requires high-level TCR signal input. Rac and p38 activation depends on SOS1 expression but not allosteric activation. Based on computational predictions and experiments exploring whether SOS functions as a RacGEF or adaptor in Rac-p38 activation, we established that the presence of SOS1, but not its enzymatic activity, is critical for p38 activation.

Mitogen-activated protein kinase (MAPK) signaling cascades are conserved pathways that can be activated by a wide variety of stimuli and play a role in diverse cellular processes (1). Early on, it was recognized that activation of the extracellular signal-regulated kinase (ERK) MAPK can be graded or switch-like, and this impacts biological outcome (2). Specifically, stimulation of rat adrenal pheochromocytoma (PC-12) cells with neuronal growth factor (NGF) results in sustained activation of the MAPK ERK and differentiation, whereas stimulation with epidermal growth factor (EGF) elicits transient ERK activation and cell proliferation (2). Synthetic engineering to rewire the feedback loops in the NGF- and EGF-ERK networks alters cell fate, further demonstrating a causative link between the mode of ERK activation and the cell biological effect (3). Individual *Xenopus* oocytes demonstrate a very large Hill coefficient for ERK activation, and ERK functions as an ultrasensitive switch to convert graded progesterone stimuli into all-or-none biological responses (4). Various mechanisms have been described to account for the switch-like ERK activation, including high cooperativity intrinsic to the ERK module (5, 6), signal amplification toward digital patterns in Ras nanoclusters (7), a dual negative feedback control by phosphatase SHP1 (8), and subcellular location of cascade activity (9).

T cells can also convert analog receptor input into digital or bimodal ERK activation (8, 10–12). Developing thymocytes must undergo all-or-none selection processes to retain functional T cells but delete autoreactive T cells (13). The small GTPase Ras in the Ras-RAF-MEK-ERK pathway (14, 15) plays a critical role during thymocyte selection (16). At least two families of Ras guanine nucleotide exchange factors (RasGEFs) establish T cell receptor (TCR)-induced GTP loading of Ras in thymocytes, namely, RasGRP and SOS (17). RasGRP1 plays a nonredundant role in Ras-ERK pathway activation; positive selection of thymocytes and

TCR-induced ERK phosphorylation is impaired in *Rasgrp1*$^{-/-}$ mice (18). Similarly, deletion of RasGRP1 and RasGRP3 in the chicken DT40 model B cell line greatly impairs B cell receptor (BCR)-induced ERK activation (19, 20). SOS RasGEFs are recruited to the plasma membrane via the small adapter molecule Grb2 (21, 22). In addition to other forms of regulation, SOS1's catalytic activity critically relies on an allosteric binding pocket for Ras previously identified in SOS1's crystal structure (23). Efficient binding of RasGTP to this pocket induces a conformational switch to enhance SOS1's GEF activity (24). We previously demonstrated that RasGRP1 alone sends analog ERK signals (10, 12, 25). We also proposed that positive feedback regulation of SOS enables bimodal, TCR-/BCR-triggered ERK activation through a mechanism that involves allosteric activation of SOS by RasGTP (10, 12, 25).

Results from several studies, including our own, have culminated in a model for discriminatory thymocyte selection signals that is based on modest analog TCR-ERK signals via RasGRP driving positive selection and strong digital SOS-ERK signals via SOS establishing negative selection (reviewed in references 13 and 26). In agreement with this model, RasGRP1 without SOS sends ana-

log ERK signals (10, 12, 25), ERK phosphorylation and positive selection are impaired in *Rasgrp1*$^{-/-}$ mice (18), ERK1 and ERK2 doubly deficient thymocytes demonstrate impaired positive selection (27), and *Grb2* haploinsufficiency (28) or conditional inactivation of *Sos1* (29) in thymocytes leaves positive selection intact. However, recent studies have demonstrated that this model is incomplete; negative selection is intact in ERK1$^{-/-}$ ERK2$^{-/-}$ thymocytes (30) as well as in thymocytes with conditional inactivation of *Sos1* (29), even in the context of SOS2 deletion (31). Thus, TCR-induced digital ERK activation alone cannot be sufficient for the negative selection signal.

A modified model explaining the TCR-induced opposing fates of developing thymocytes, life or death, has been put forth on the basis of differential activation of the ERK, p38, and Jun N-terminal protein kinase (JNK) MAPK pathways (13, 26). In support of this model, pharmacological inhibition of p38 MAPK blocks negative selection of thymocytes in fetal thymic organ cultures (32), and p38 and JNK activation and negative selection are impaired in *Grb2* heterozygous mice (28). However, the molecular mechanisms of p38 and JNK activation pathways in lymphocytes are largely unknown (33, 34).

The above-mentioned studies motivated us to explore how RasGEFs might coordinate activation of different MAPK pathways. We took an approach that combined synergistic computer simulations and biochemical assays using model cell lines and primary thymocytes to examine the role of SOS in regulating the quantity and quality of Ras and MAPK signal output. Here we demonstrate that highly sensitive digital ERK activation requires allosteric activation of SOS in lymphocytes and that RasGRP is an important catalyst for ERK activation. Antigen receptor-stimulated activation of the Rac-p38 pathway depends on SOS1 more than it does on RasGRP1. In contrast to ERK activation, optimal p38 activation does not critically depend on positive feedback regulation via SOS1's allosteric pocket. In addition, p38 activation was not affected by enzymatic crippling of SOS1's RasGEF or Dbl domain, implying that SOS1 functions as an adapter in the p38 pathway. These results show a stark contrast between the mechanisms of ERK and p38 activation and propose new hypotheses for the role of SOS in MAPK activation in selecting thymocytes. We also anticipate that our studies will be applicable to SOS function in other cell types, downstream of other receptor systems like the epidermal growth factor receptor (EGFR).

MATERIALS AND METHODS

Cell lines, mice, stimulations, and inhibitor treatment. Cultures of human Jurkat leukemic T cells, chicken DT40 cell lines, and DT40-derived lines were maintained as described previously (10, 19, 20). All experimental mice were used at the age of 6 to 7 weeks. Age- and sex-matched major histocompatibility complex type I and II (MHCI/II)-double-deficient (Abb/β2m) mice were purchased from Taconic (Hudson, NY). For cell stimulation, harvested cells were rested for 30 min in phosphate-buffered saline (PBS) or plain RPMI at 37°C. For phospholipase Cγ (PLCγ) inhibition, cells were preloaded for 20 min with U73122 inhibitor (Calbiochem) or its inactive analog U73343 at 5 μM (Calbiochem). Stimulations of DT40 cells were carried out in PBS or plain RPMI at 37°C with the indicated doses of M4 anti-BCR antibody hybridoma ascites fluid preparation.

Hartigan's analysis. We previously employed Hartigan's statistical analyses of phospho-ERK (pERK) histograms to label them as unimodal or bimodal (10). Here we used the average of cell counts in the neighboring five gates to smooth the cell count data in each gate in the pERK flow

TABLE 1 Concentrations used for each species

Species	Concn (no. of molecules/simulation box)
LAT	200
PLCγ-RasGRP	100
Grb2-SOS	100
Gads	100
Rac	1,000
p38	1,000

cytometry experiment. We repopulated the pERK levels uniformly within each gate to generate a continuous distribution of pERK expression patterns and applied Hartigan's test to the generated distribution.

Computer modeling. For Fig. 2, we used an established computational model of Ras activation via receptor input, as described in Fig. 1A of Riese et al. (35), with the extension of the Ras-Raf-MEK-ERK activation cascade (36), as depicted in Fig. S1 in the supplemental material. In this model, SOS1 and SOS2 are represented by SOS, i.e., we do not make a distinction between SOS1 and SOS2 in the model. To further explore the effects of downstream regulation of Ras activation, we included negative and positive feedback loops, as depicted in Fig. S2 in the supplemental material. We used our implementation of the standard Gillespie algorithm (37), the stochastic simulation compiler (SSC), to simulate the described signaling network stochastically. In all stochastic simulations, we used a spatially homogeneous simulation box with size V of area (4 mm^2) times height (0.02 mm). This choice of the system size ensures that the system is well mixed. The initial concentrations and the rate constants are those in Tables S1 to S4 of Das et al. (10), Tables 1 and 2 of Riese et al. (35), and the supplemental material of Locasale et al. (36), except we used 36 molecules/μm^2 for PIP$_2$ to match published results (35). More details of the choice of parameters can be found in the supplemental materials of Das et al. (10) and Riese et al. (35).

For the results shown in Fig. 8, we also performed stochastic simulations to investigate Rac activation when SOS functions directly as a RacGEF and/or functions as an adaptor recruiting and stabilizing RacGEF at the LAT signalosome. We assumed that a threshold level of active Rac would be needed for p38 activation. To mimic such a thresholding behavior, we modeled p38 activation kinetics as second order in the amount of active Rac, which is equivalent to a Hill coefficient of two for p38 activation. The detailed model specification and parameter choice are indicated here. We made the following assumptions in the coarse-grained models: (i) the LAT signalosome, possibly through Gads, activates RacGEF, and (ii) RasGRP, possibly recruited by PLCγ, stabilizes the LAT signalosome and hence regulates RacGEF. In all Gillespie simulations, we used a spatially homogeneous simulation box with a size V of area (4 mm^2) times height (0.02 mm). All the rate parameters reported below have the unit of s^{-1}, which is directly used in the simulations; all the species concentrations reported below have the unit of number of molecules per simulation box. For SOS-deficient, RasGRP-deficient, and SOS DH-PH mutant cases, the SOS concentration, RasGRP concentration, and rate of Rac activation by SOS (if it exists), respectively, are set to zero (Table 1).

Case 1. SOS functions as both a RacGEF and an adaptor. When both Grb2-SOS and PLCγ-RasGRP bind to LAT, the LAT signalosome complex is more stable and more effective in activating Rac. Grb2-SOS, when bound to LAT, activates Rac directly (Table 2).

Case 2. SOS functions as an adaptor only. Grb2-SOS binding to LAT stabilizes the LAT signalosome complex and increases its RacGEF activity; PLCγ-RasGRP's binding further enhances such cooperativity. Grb2-SOS does not activate Rac directly (Table 3).

Case 3. SOS functions as a RacGEF. Grb2-SOS, when bound to LAT, activates Rac directly. RasGRP, when bound to the LAT signalosome, cooperatively enhances SOS's RacGEF. Rac can also be activated via a Gads-mediated pathway, but SOS's binding to LAT does not contribute to it (Table 4).

TABLE 2 Case 1: SOS functions as both a RacGEF and an adaptor[a]

Reaction	k_{on} (1/s)	k_{off} (1/s)	k_{cat} (1/s)
Gads binding to and unbinding from LAT without cooperativity	0.1	5	
Grb2-SOS binding to and unbinding from LAT	0.12	0.8	
PLCγ-RasGRP binding to and unbinding from LAT	0.16	0.5	
Gads unbinding from LAT bound with SOS and RasGRP		0.01	
SOS activating Rac			0.008
Gads activating Rac without cooperativity			0.005
Gads activating Rac with cooperativity			0.1
Rac self-decaying to inactive form			80
Rac activating p38			1
p38 self-decaying to inactive form			35

[a] When both Grb2-SOS and PLCγ-RasGRP bind to LAT, the LAT signalosome complex is more stable and more effective in activating Rac. Grb2-SOS, when bound to LAT, activates Rac directly.

Plasmids and stable and transient transfection. Plasmid expressing full-length hSOS1 with a DBL domain mutation (pEF6-hSOS1 DBL[mut]) was constructed by modifying pEF6 hSOS1 wild type (WT) with 7 amino acid substitutions (LHYFELL to IIIRDII) (38). Other plasmids and the small interfering RNA (siRNA) duplex used in this study were described previously (10, 20, 39). For transient cotransfection of hSOS1 with the hCD16/7 fusion construct, 300 μl of SOS1⁻ SOS2⁻ DT40 cell suspension at 66 × 10⁶ cells/ml in plain RPMI was electrotransfected with 10 μg of each plasmid by using a Bio-Rad electroporator (Bio-Rad) set at square wave, 300 V, with a 10-ms single pulse. Transfected cells were cultured for 16 to 20 h prior to phospho-flow assay or to anti-hCD16-biotin magnetically activated cell sorting (MACS) purifications by following the manufacturer's guidelines (Miltenyi Biotec). For stable reconstitution of human SOS1, SOS1⁻ SOS2⁻ DT40 cells were transfected with 10 μg hSOS1 plasmid by electroporation set at exponential decay, 250 V, 950 μF. Transfected cells were selected by 10 μg/ml final blasticidin S (Fischer Biotech) from 24 h posttransfection. Single cell-derived clones were isolated from a set of serially diluted cultures on 96-well plates after 1 to 2 weeks of seeding. Isolated clones were screened for hSOS1 and surface BCR (sBCR) expression by Western blotting and fluorescence-activated cell sorting (FACS), respectively.

Western blot analysis of cell lysates. Levels of various proteins were measured by Western blotting as previously described (10, 20). The following antibodies were purchased from Cell Signaling: phospho-p44/42 MAPK ERK1/2 (pT204/pY204), total ERK1/2, phospho-p38 (pT180/pY182, clone 3D7), total p38, phospho-PLCγ1 (pY783), and phospho-ZAP70 (pY319). Other antibodies were human SOS1 (BD Transduction Lab), mRasGRP1 (clone m199), Grb2 (SC-255; Santa Cruz Biotech), α-tubulin (Sigma), Rac1 (clone 23A8; Millipore), and pan-Ras (clone Ab-3; Calbiochem) for detection of chicken Ras. Proteins were visualized using enhanced chemiluminescence (ECL) Western blot substrate (Pierce) and the LAS-4000 image system (Fujifilm Life Science). Densitometric analysis was performed using Multi Gauge V3.0 (Fujifilm Life Science). Shown results are representative of two or more independent experiments.

Intracellular FACS staining for pERK, phospho-p38, and hSOS1. BCR-induced MAPK activation and hSOS1 protein levels were measured by intracellular FACS staining as previously described (10). In brief, DT40 cells were resuspended/rested in PBS or plain RPMI at 2.0 × 10⁶ cells/75 μl (per well of a 96-well plate). Cells were stimulated for the desired amount of time by adding 75 μl of 2× stimulation mix and subsequently fixed for 20 min at room temperature by mixing with 150 μl fixation buffer (Cytofix/Cytoperm; BD Biosciences). Cells were washed and permeabilized for at least 30 min with 90% methanol at −20°C. Fixed/permeabilized cells were stained with anti-phospho-p44/42 MAP kinase (Thr202/Tyr204) antibody (number 9101; Cell Signaling), phospho-p38 (pT180/pY182, clone 3D7), and anti-hSOS1 (BD Transduction Lab) at room temperature (RT) in the presence of 2% (vol/vol) normal goat serum (Jackson ImmunoResearch Laboratories). Subsequently, cells were washed twice and stained with phycoerythrin (PE)- or allophycocyanin (APC)-conjugated AffiniPure F(ab′)₂ fragment donkey anti-rabbit IgG (Jackson ImmunoResearch Laboratories) with Alexa Fluor 488-conjugated donkey anti-mouse IgG antibody (Invitrogen). Stained cells were washed 3 times and directly analyzed by FACS.

Ras and Rac activation assays. BCR-induced Ras and Rac activation were analyzed by Ras/RacGTP pulldown assays according to the manufacturer's instructions (Upstate).

TABLE 3 Case 2: SOS functions as an adaptor only[a]

Reaction	k_{on} (1/s)	k_{off} (1/s)	k_{cat} (1/s)
Gads binding to and unbinding from LAT without cooperativity	0.1	5	
Grb2-SOS binding to and unbinding from LAT	0.12	0.8	
PLCγ-RasGRP binding to and unbinding from LAT	0.16	0.5	
Gads unbinding from LAT bound with RasGRP only		5	
Gads unbinding from LAT bound with SOS only		0.05	
Gads unbinding from LAT bound with SOS and RasGRP		0.01	
Gads activating Rac without cooperativity			0.005
Gads activating Rac when LAT bound with RasGRP only			0.005
Gads activating Rac when LAT bound with SOS only			0.015
Gads activating Rac when LAT bound with SOS and RasGRP			0.1
Rac self-decaying to inactive form			80
Rac activating p38			1
p38 self-decaying to inactive form			30

[a] Grb2-SOS binding to LAT stabilizes the LAT signalosome complex and increases its RacGEF activity; PLCγ-RasGRP's binding further enhances such cooperativity. Grb2-SOS does not activate Rac directly.

TABLE 4 Case 3: SOS functions as a RacGEF[a]

Reaction	k_{on} (1/s)	k_{off} (1/s)	k_{cat} (1/s)
Gads binding to and unbinding from LAT without cooperativity	0.1	5	
Grb2-SOS binding to and unbinding from LAT without cooperativity	0.12	0.8	
PLCγ-RasGRP binding to and unbinding from LAT	0.16	0.5	
Grb2-SOS unbinding from LAT bound with RasGRP		0.01	
Gads activating Rac			0.007
SOS activating Rac when LAT bound with RasGRP			0.05
SOS activating Rac when LAT unbound with RasGRP			0.0045
Rac self-decaying to inactive form			80
Rac activating p38			1
p38 self-decaying to inactive form			20

[a] Grb2-SOS, when bound to LAT, activates Rac directly. RasGRP, when bound to the LAT signalosome, cooperatively enhances SOS RacGEF. Rac can also be activated via a Gads-mediated pathway, but SOS binding to LAT does not contribute to it.

RESULTS

Robust ERK activation occurs in thymocytes and requires both RasGRP and SOS. It has been suggested that thymocytes require low levels of TCR signal input to activate ERK but higher levels of TCR stimulation to also activate p38 and JNK ([13], [34], [40]). To test this, we stimulated total thymocytes from mice with a low or high dose of anti-CD3ε cross-linking antibody. ERK phosphorylation was robustly induced by low levels of TCR stimulation, whereas phosphorylation of p38 was more modest and critically depended on a high dose of stimulating anti-CD3ε antibody. Phosphorylation of JNK was efficiently induced by sorbitol but was not triggered by CD3ε cross-linking (Fig. 1A). Similarly, wild-type chicken DT40 B cells activate ERK in a very sensitive manner,

following anti-BCR stimulating antibody (M4). The presence of both RasGRP and SOS RasGEFs is required for triggering high levels of ERK activation at the population level, measured by Western blotting (Fig. 1B). These results in DT40 cells are in agreement with the reported ERK activation impairment in $Rasgrp1^{-/-}$ ([41]), $Sos1^{-/-}$ ([29]), and $Sos1^{-/-} Sos2^{-/-}$ ([31]) thymocytes. We previously reported that bimodal ERK activation disappears in the absence of SOS1/SOS2 ([10]). We expanded on these findings by performing extensive time courses and dose responses. As before ([10]), mean fluorescence values of ERK phosphorylation data points were used as input for Hartigan's analyses. Here we further increased the stringency of these Hartigan's analyses so that ERK phosphorylation was termed bimodal (B) only when a
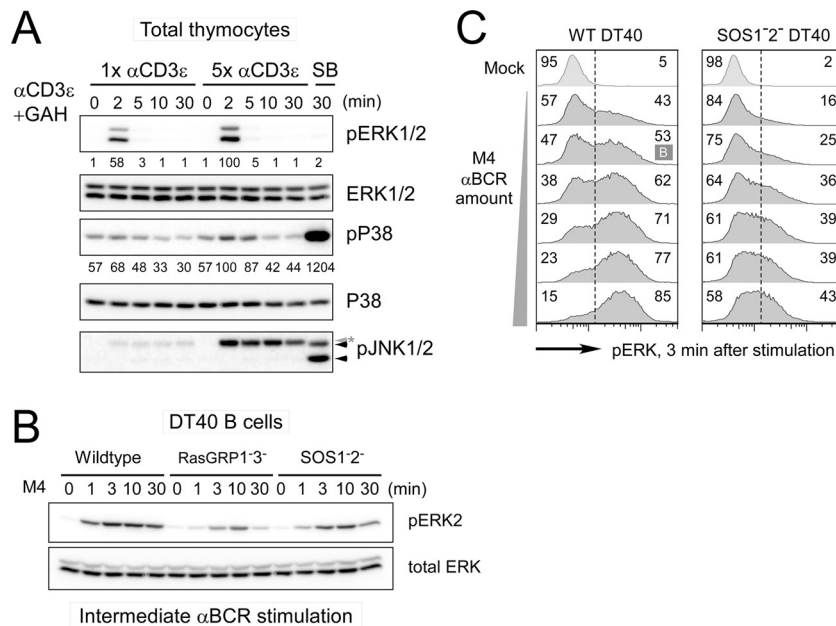

FIG 1 The MAPK ERK activation pattern depends on stimulus dosage and SOS. (A) Activation of MAPK ERK and p38 in total mouse thymocytes induced with 1× (2 µg/ml) and 5× (10 µg/ml) αCD3ε (2C11) stimulation. SB, 30-min stimulation with 0.4 M sorbitol as a positive control for phospho-p38 (pP38) and phospho-JNK1/2 (pJNK1/2; arrowheads). The asterisk indicates a heavy chain of stimulatory antibody. (B) Deficiency in either RasGRP or SOS leads to impaired ERK activation in DT40 cells. Wild-type, RasGRP1⁻ RasGRP3⁻, and SOS1⁻ SOS2⁻ DT40 cells were activated with an intermediate dosage of M4 anti-BCR stimulation for the indicated time. (C) SOS1/2-deficient DT40 cells do not demonstrate a bimodal pERK pattern after 3 min of BCR stimulation, regardless of the strength of the BCR stimulus (dilution range, 1:32,000 to 1:1,000). Bimodality is statistically tested by Hartigan's analysis. A case with lower than the threshold dip value in Hartigan's unimodality test ($P < 0.05$) is classified as bimodal (indicated as B), while cases with a P value of >0.05 are considered unimodal. Numbers represent the percentage ratios of maximum phosphoprotein levels normalized to total levels of that specific protein. All data are representative presentations of at least three independent experiments.
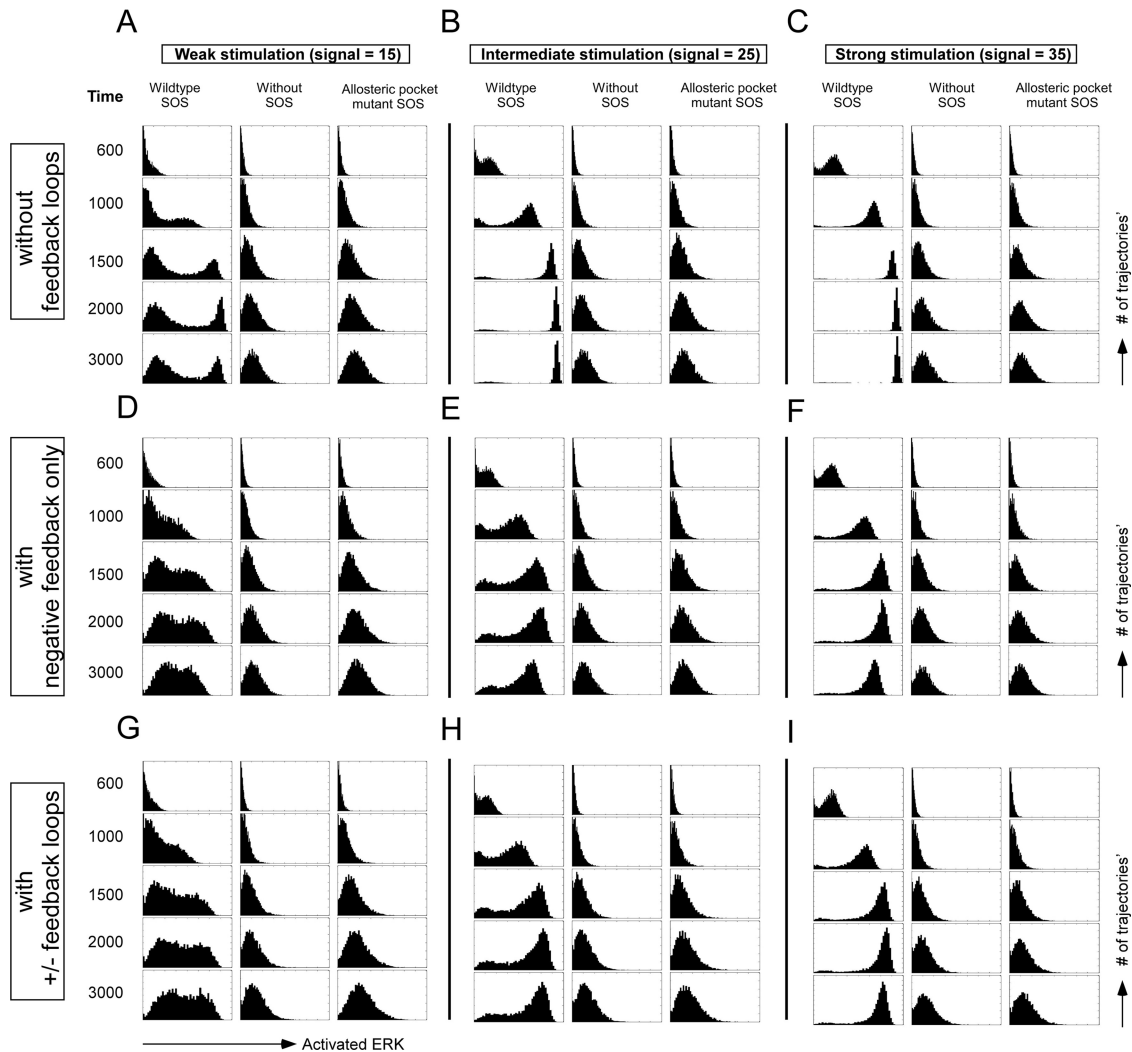
FIG 2 *In silico* prediction of ERK activation patterns under weak, intermediate, or strong stimulations. ERK activation in cells with wild-type SOS, without SOS, or with allosteric mutant W729E SOS expression is projected at increasing time points. Each plot is a histogram of 8,000 realizations from stochastic simulations. (A to C) In the simulations, there is no negative feedback loop from ERK to SOS or positive feedback loop in the RAF-MEK-ERK module. (D to F) The negative feedback loop from ERK to SOS is added. (G to I) The simulations include both the negative feedback loop from ERK to SOS and the modest positive feedback loop in the RAF-MEK-ERK module.

default null hypothesis of unimodal phospho-ERK (pERK) patterns is rejected. As such, we established that BCR stimulation-induced ERK activation is not bimodal for any dose or at any time point when SOS RasGEFs are missing (Fig. 1C). We hypothesized that the lack of bimodal ERK activation in SOS-deficient cells is caused by the absence of the allosteric feedback to SOS.

***In silico* modeling: allosteric activation of SOS1 is required for bimodal ERK activation.** To test our hypothesis, we extended our previous computational models for Ras activation to include ERK activation downstream of Ras and carried out stochastic computer simulations of the Ras-ERK signaling cascade (10, 35, 36). Thus, we explored the effect of SOS, in particular, the SOS allosteric pocket, in ERK activation. By altering the computational parameters depicted in Fig. S1 in the supplemental material, we modeled ERK activation in cells with wild-type SOS, without SOS, or with allosteric mutant SOS as a function of time and stimulus dosage. We predicted ERK activation profiles at different time

points with three different stimulus levels, namely, (i) weak, (ii) intermediate, and (iii) strong stimulation. These stochastic simulations predict that bimodal ERK activation will occur in cells with wild-type SOS but that bimodality will disappear when SOS is absent or when SOS cannot be allosterically activated, regardless of dosage level or stimulation time (Fig. 2A to C).

The output through the SOS-Ras-RAF-MEK-ERK pathway is influenced by feedback regulation with both negative and positive feedback loops connecting to ERK and SOS. The exact nature of negative feedback loops is not understood, and there appear to be differences between lymphoid and nonlymphoid (epithelial) cell lineages (42–45). To explore the negative feedback to SOS, we modified our model to include these parameters (46), the phosphorylation rate of SOS1 by pERK, $k_p = 0.02$ s^{-1} μM^{-1}, and the dephosphorylation rate of pSOS1, k_d. The process of dephosphorylation of pSOS1 is extremely slow; we therefore take k_d as 0 s^{-1} μM^{-1} here (see Fig. S2 in the supplemental material). Inclusion of
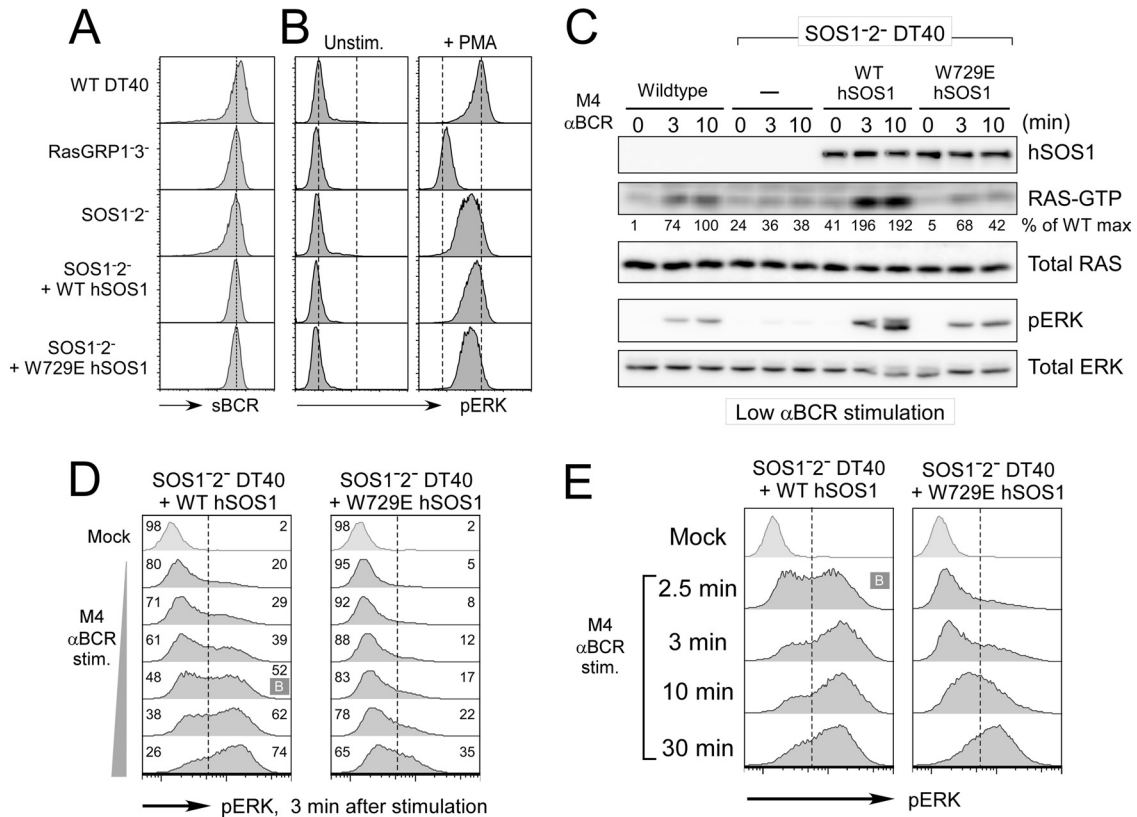
FIG 3 Efficient and bimodal Ras-ERK signaling requires an intact allosteric pocket in SOS1 (W729). (A) Surface BCR levels of various DT40 cell lines. SOS1/2-deficient DT40 cells stably reconstituted with wild-type (WT; clones 1 to 9) or allosteric mutant W729E (clones 2 to 9) hSOS1 express surface BCR levels comparable to those of wild-type and other mutant DT40 cells. (B) Various DT40 B cell lines were stimulated with 25 ng/ml PMA for 10 min. MAPK ERK activation is measured by phospho-flow cytometry. Two dashed lines indicate unstimulated and PMA-induced levels of phospho-ERK in wild-type DT40 cells. (C) BCR-induced Ras and ERK activation depends on SOS and on SOS's allosteric pocket. Various DT40 cells were stimulated with a low dose of M4 anti-BCR antibody and analyzed as in Fig. 1B. Part of the lysates was used to assay BCR-induced Ras-GTP accumulation. Percentages relative to the wild-type maximum activation are shown. (D and E) Reconstitution of SOS1⁻ SOS2⁻ DT40 cells with the W729E hSOS1 does not lead to rescue of the bimodal pERK pattern, regardless of dose or time course of stimulation. Bimodality statistically supported by Hartigan's analysis is marked with "B" as in Fig. 1C. Presented data are representative of at least three independent experiments.

these feedback loops does not change the overall qualitative behavior of our stochastic models that explore the wild-type, no-SOS1, and lack-of-allosteric-activation-of-SOS situations. The main new effect is that the activated ERK levels begin to decline at longer times (Fig. 2D to F). We next expanded our model to include a positive feedback loop in the RAF-MEK-ERK module (47). The exact rate, or strength, of positive feedback regulation is not known, so we varied these parameters. For weak positive feedback regulation, there is no effect, whereas for very strong positive feedback, all trajectories shifted to maximal ERK phosphorylation very rapidly (data not shown). For moderate positive feedback regulation, which seems physiologically realistic, we still find bimodal ERK responses only for the wild-type SOS. But the bimodality is less sharply defined, with more simulation trajectories "caught" between the on and off states at any given time point (Fig. 2G to I). Notice that these simulation results resemble the experimental results more closely than if feedback regulation is not included.

Disruption of SOS1's allosteric activation negates bimodal Ras-ERK activation. Based on the structure of SOS1, tryptophan residue 729 (W729) was identified as a key residue coordinating Ras binding within the allosteric pocket (23, 48). A single-amino-

acid alteration of tryptophan into glutamic acid (W729E) cripples allosteric activation of nucleotide exchange activity of the isolated catalytic domain of SOS1 in vitro and in transfected cells (10, 48). To directly test our predictions from the simulations in Fig. 2, we stably reconstituted SOS1⁻ SOS2⁻ DT40 cells with either WT or W729E (allosteric pocket mutant) human SOS1 (hSOS1). Selected stable clones, WT DT40 and DT40 mutants, expressed comparable levels of surface BCR (sBCR) (Fig. 3A), and WT and W729E hSOS1 proteins were expressed at comparable levels as well (Fig. 3C). We first analyzed Ras and ERK activation at the population levels and established that WT hSOS1 reconstitution rescued the BCR-induced Ras and ERK activation defect in SOS1⁻ SOS2⁻ DT40 cells. In contrast, W729E hSOS1-reconstituted cells demonstrated significantly lower levels of activated Ras and ERK than the WT hSOS1 stable clone (Fig. 3C). WT hSOS1-reconstituted SOS1⁻ SOS2⁻ DT40 cells demonstrated slightly enhanced responses compared to parental DT40 cells. This may be a reflection of differences between chicken and human SOS1. Alternatively, hSOS1 may be expressed at higher levels than chicken SOS1, but lack of a cross-reactive SOS1-specific antibody prevented us from testing this. WT and W729E hSOS1-reconstituted cells were therefore directly compared in the following experi-
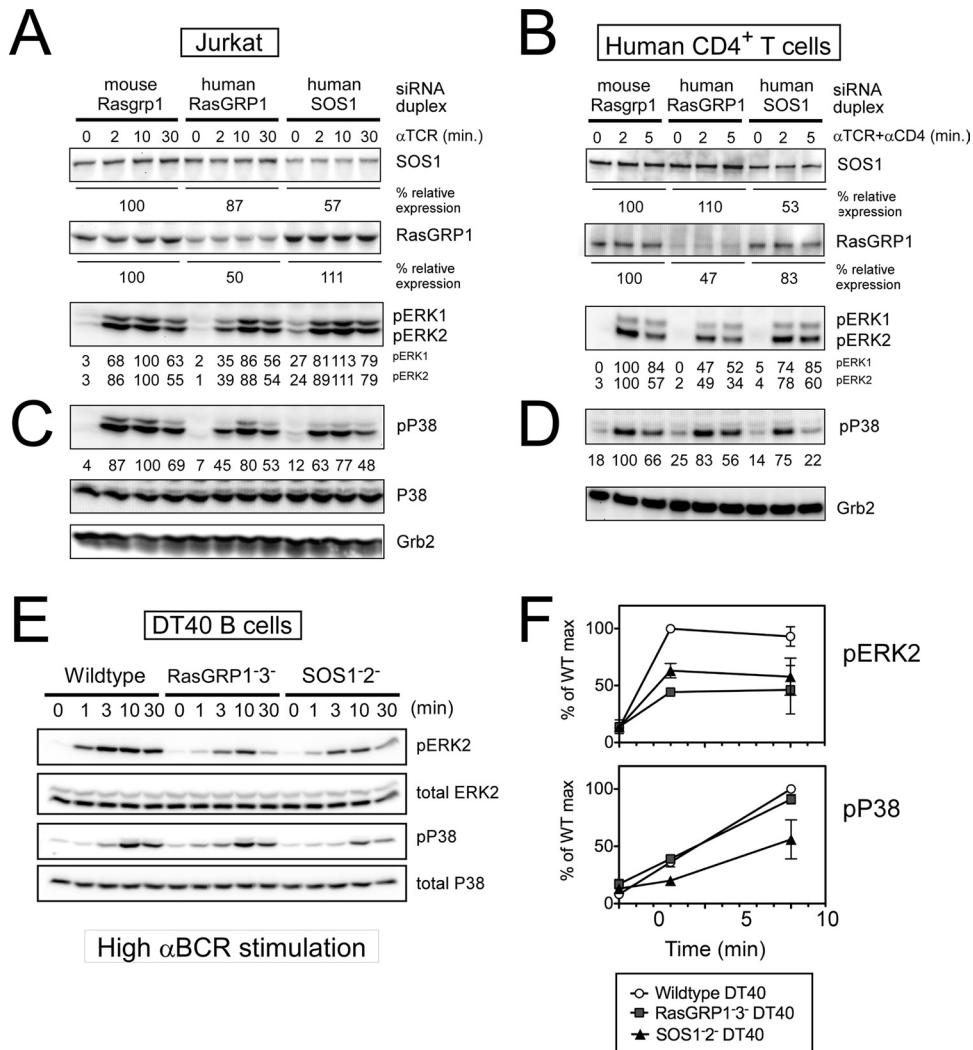
FIG 4 Optimal p38 activation preferentially requires SOS1. (A to D) siRNA-driven knockdown of SOS1 in Jurkat T cells (A and C) or in human peripheral blood CD4+ T cells (B and D) results in a reduction of TCR-triggered p38 activation that is more pronounced than when RasGRP1 expression levels are reduced by siRNA-driven knockdown. (A and B) Partial reproduction of Fig. 2B and C in Roose et al. (20), and experimental details are described there. Mouse RasGRP1-specific siRNA duplex was used for off-target effect control in both experiments. Residual expression levels of SOS1 and RasGRP1 are represented as percentages of the control level. Representative of three independent experiments. (E and F) Impaired BCR-induced p38 activation in the absence of SOS. Wild-type and mutant DT40 cells were stimulated with a high dosage of M4 anti-BCR antibody for the indicated time. Percentages relative to the wild-type maximum response of pERK and phospho-p38 normalized to each total protein level are plotted in panel F. Data are means ± standard deviations (SD) from four independent experiments.

ments. Significantly, BCR stimulation of WT hSOS1-reconstituted SOS1− SOS2− cells resulted in a rescue of the bimodal ERK activation pattern, revealed by dose responses and time courses of BCR-induced phospho-ERK flow cytometry and Hartigan's analyses of the resulting phospho-ERK histograms (Fig. 3D and E). In contrast, bimodal ERK activation was never observed in W729E hSOS1-reconstituted SOS1− SOS2− DT40 cells regardless of stimulation dose or time (Fig. 3D and E). Expression of W729E hSOS1 did not lead to a general impairment of ERK activation, as strong stimulation of cells with phorbol myristate acetate (PMA) (a synthetic analog of diacylglycerol [DAG]) resulted in very similar ERK activation in WT DT40, SOS1− SOS2− WT hSOS1, and SOS1− SOS2− W729E hSOS1 cells (Fig. 3B). Likewise, the observed results did not reflect uniquely selected stable clones; additional WT and W729E hSOS1 stable clones were tested in parallel

and exhibited similar dynamics and patterns of BCR-induced pERK (data not shown).

Optimal p38 activation preferentially requires SOS1. Pharmacological inhibition of p38 MAPK blocks negative selection of thymocytes in fetal thymic organ cultures (32). In $Grb2^{+/-}$ thymocytes, TCR-induced p38 activation is impaired (28), suggestive of a possible role for SOS RasGEFs that are recruited by Grb2, but TCR-induced p38 activation has not been examined in $Sos1^{-/-}$ (29) or $Sos1^{-/-}$ $Sos2^{-/-}$ thymocytes (31) to date or in $Rasgrp1^{-/-}$ thymocytes (41). We previously reported how RasGRP1 plays a more dominant role in ERK activation in TCR-stimulated Jurkat T cells or human CD4+ T cells than SOS1 (20) (Fig. 4A and B). To address how these RasGEFs might affect the p38 MAPK pathway and how this compares to their roles on the ERK pathway, we determined TCR-induced p38 activation in the exact same sam-
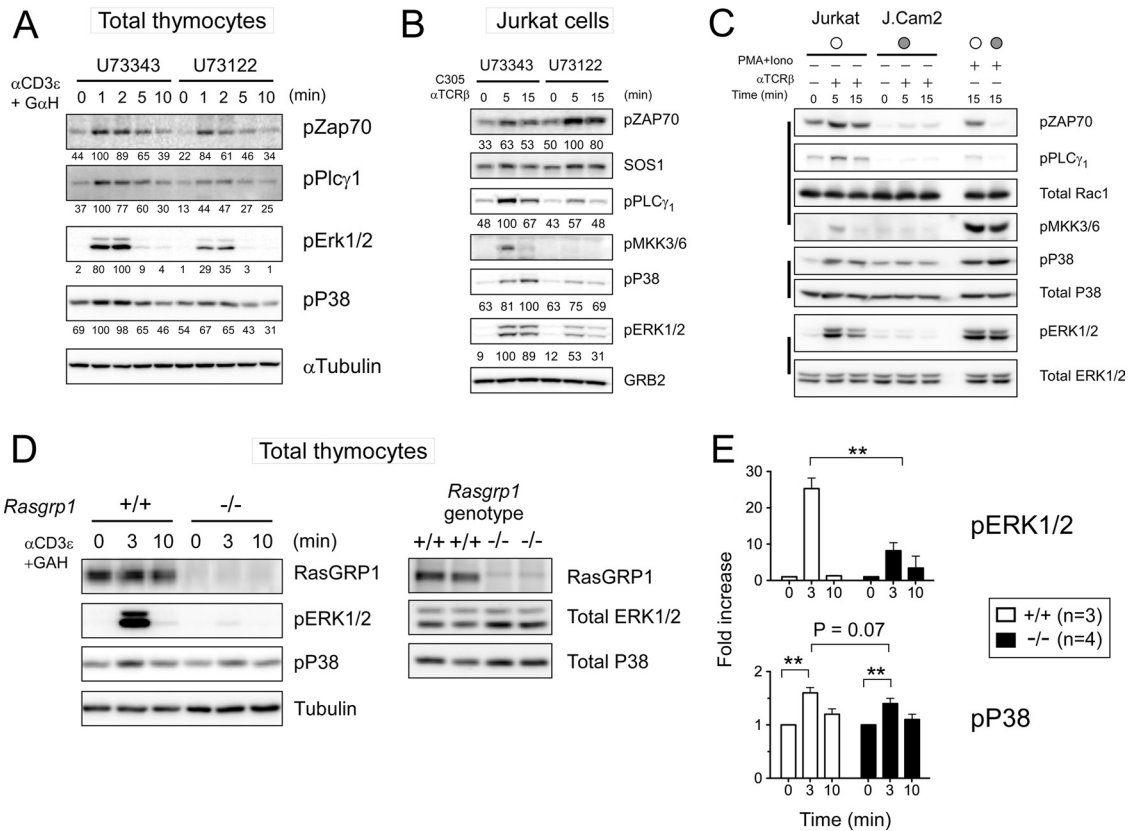
FIG 5 The PLCγ-RasGRP1 axis contributes only minimally to p38 activation in thymocytes. (A and B) Pharmacological inhibition of DAG-producing PLCγ by U73122 results in a modest reduction of p38 activation compared to the reduction in ERK activation in TCR-stimulated total thymocytes and Jurkat cells. U73343, inert analog, is used as a treatment control. Percentages relative to the control maximum activation are shown. Representative of two experiments. (C) TCR-stimulated MKK3/6 and p38 activation is compared between wild-type and LAT-deficient J.Cam2 Jurkat cells. (D and E) Minute reduction in TCR-induced p38 activation in *Rasgrp1*-deficient thymocytes. Control *Rasgrp1*^{+/+} thymocytes were obtained from MHCI/II double-deficient mice. Data are means ± SD from at least three mice of each genotype (Student *t* test; *, $P < 0.05$; **, $P < 0.01$).

ples in which RasGRP1 or SOS1 expression was targeted by siRNA duplexes. We found that the role of RasGRP1 in p38 activation is more modest than that for ERK activation. However, TCR-induced activation of p38 was consistently more impaired by reduced SOS1 expression than by a similar level of reduced RasGRP1 expression in both Jurkat T cells and human CD4^{+} T cells (Fig. 4C and D). These siRNA approaches yield only partial knockdown of RasGRP1 or SOS1. To determine the effects under complete absence of RasGRP-1 and -3 or of SOS-1 and -2, we turned to our RasGRP1^{−} RasGRP3^{−} and SOS1^{−} SOS2^{−} DT40 cell lines, which substantiated the siRNA findings; the SOS RasGEFs made a larger contribution toward BCR-induced p38 activation than the RasGRP RasGEFs, whereas the opposite holds true for activation of ERK (Fig. 4E and F). Given the differential contribution of RasGRP and SOS to ERK versus p38 activation and that p38 activation is not sharply thresholded as in the digital ERK activation, we hypothesized that activation of ERK and p38 in thymocytes occurs in a mechanistically different way downstream of these RasGEFs.

Modest contribution from the PLCγ-RasGRP1 axis to thymocyte p38 activation. We first utilized a pharmacological approach to inhibit phospholipase C (PLC) with U73122, the enzyme that produces the second messengers IP$_3$ and DAG. The latter is essential for RasGRP1 membrane recruitment and activa-

tion in thymocytes and T cell lines (17). As expected based on the established role of the DAG-RasGRP1-Ras pathway for ERK activation, exposure of total mouse thymocytes and Jurkat cells to U73122 reduced the maximal induction of ERK activation by 65% and 47%, respectively, following TCR stimulation compared to that of cells treated with inert analog U73343 as a control (Fig. 5A and B). In contrast, U73122 treatment in thymocytes had a more modest effect (reduction by 33%) on the TCR-induced activation of p38 (Fig. 5A and B). U73122 had a small effect on proximal TCR signals, evidenced by the small decrease in phosphorylation of ZAP70 (Fig. 5A). Jurkat cells show delayed kinetics of TCR-induced p38 activation compared to mouse and human primary T cells (Fig. 4C and D) (data not shown). U73122 treatment of Jurkat cells only minutely affected TCR-induced p38 activation, especially at 5 min, while the impact at the later time point was greater (reduction by 31% at 15 min) (Fig. 5B). Interestingly, ZAP70 activation was not reduced in U73122-treated Jurkat cells, while the upstream MKK3/6 activation was completely abolished (Fig. 5B). Activation of p38 downstream of the TCR has been described to occur via LAT-dependent classical and LAT-independent alternative pathways (49). It is possible that the difference between thymocytes and Jurkat cells comes from different contributions of classical and alternative p38 pathways. To examine the contribution of the LAT-independent pathway in our own hands,
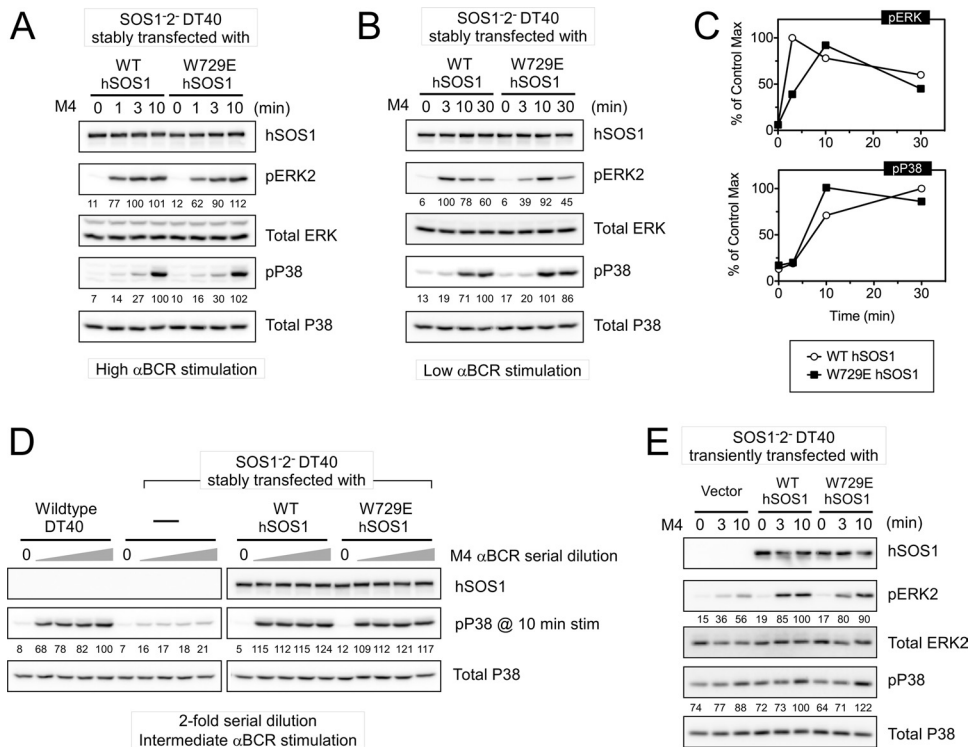
FIG 6 SOS1's allosteric pocket is dispensable for optimal p38 activation. (A, B, and C) W729E hSOS1 and WT hSOS1 similarly rescue the SOS1⁻ SOS2⁻ DT40 cells in terms of p38 activation regardless of stimulus dosage. Quantitation of pERK and phospho-p38 signals relative to the maximum WT control level is plotted in panel C. Note that the ERK activation defect in W729E hSOS1-reconstituted cells is most noticeable with low anti-BCR stimulation. (D) p38 activation at 10 min of stimulation is measured in response to a 2-fold serial dilution of anti-BCR antibody at a range of intermediate dosages. (E) SOS1⁻ SOS2⁻ DT40 cells were transiently transfected with empty vector, WT hSOS1, or W729E hSOS1 and stimulated as indicated. Transfected cells were magnetically purified by positive selection of cotransfected human CD16/7 fusion protein. Numbers for phospho-ERK and -p38 are generated by taking the ratios of pERK/ERK and phospho-p38/p38 in the individual samples and setting the maximum phosphoprotein level in the wild-type control to 100%. Representative blots of at least three experiments.

we compared wild-type Jurkat and LAT-deficient J.Cam2 cells (Fig. 5C). In contrast to what has been reported (50), we did not see any significant TCR-induced p38 activation in J.Cam2 cells, whereas we confirmed the earlier documented (50) elevated baseline p38 phosphorylation in this cell line. It should be noted that we examined dual T180/Y182 p38 phosphorylation in our study presented here. There is some evidence that the alternative p38 pathway preferentially involves monophosphorylation of T180 (51), although T180 p38 monophosphorylation following extensive time courses and dose responses has not been explored to date.

We next took a genetic approach by comparing thymocytes from *Rasgrp1*⁻/⁻ mice with those from β2m/MHC class II doubly deficient mice. In both cases, thymocyte development is arrested, and thymi consist of a rather uniform cell population of CD4⁺ CD8⁺ thymocytes (52). In *Rasgrp1*⁻/⁻ mice, the defect is intrinsic to the thymocytes, whereas in the β2m/MHC class II doubly deficient mice, the defect lies in the epithelial cells and not in the thymocytes. ERK activation was severely impaired in TCR-stimulated CD4⁺ CD8⁺ thymocytes that are deficient for RasGRP1 (Fig. 5D and E). In contrast, the consistently modest TCR-induced p38 activation was not significantly affected by the genetic deletion of RasGRP1 (Fig. 5D and E) (P = 0.07). In summary, the mechanism of p38 activation appears to be very different from that of ERK activation, is not sharply thresholded, and is mostly independent of RasGRP1.

Allosteric activation of SOS1 is dispensable for BCR-stimulated p38 activation. Results from Fig. 4 and 5 demonstrated defective p38 activation in SOS1⁻ SOS2⁻ DT40 cells but only a minimal role for RasGRP1 in activation of the p38 MAPK. We therefore focused on the feedback loop to the allosteric pocket in SOS1 next and examined how uncoupling this loop via the W729E point mutation affects the activation of p38. Under strong BCR stimulation, the p38 activation defect in SOS1⁻ SOS2⁻ DT40 cells was restored by reconstitution with WT hSOS1 (Fig. 6A). A very similar level of restoration was obtained in SOS1⁻ SOS2⁻ W729E hSOS1 cells (Fig. 6A). Extensive time courses and dose responses revealed levels of p38 activation in W729E hSOS1-reconstituted cells that were consistently similar to those in WT hSOS1-reconstituted cells, demonstrating that the allosteric pocket in SOS1 is dispensable for optimal BCR-triggered p38 activation (Fig. 6B, C, and D). These results were further validated with transient reconstitution of SOS1⁻ SOS2⁻ cells with empty vector, WT hSOS1, or W729E hSOS1. W729E hSOS1 rescued the p38 activation defect with the same efficiency as WT hSOS1 (Fig. 6E). As a control for the impairment of allosteric activation of SOS, ERK activation was verified in all these assays. W729E hSOS1 cells always demonstrated ERK activation defects compared to WT hSOS1-expressing cells, and these defects were most pronounced under low-level stimulation conditions, reiterating the importance of allosteric activation of SOS1 for optimal ERK activation (Fig. 6A to E).

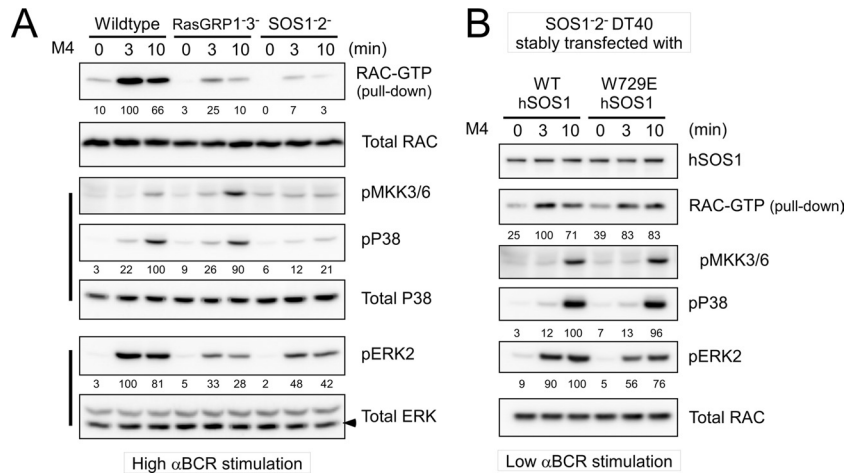**SOS1, Rac, and p38 activation.** SOS has potential dual GEF

FIG 7 BCR-induced RAC activation requires SOS but not allosteric activation of SOS1. (A) RAC activation in response to high anti-BCR dosage is measured by a RAC pulldown assay. (B) RAC activation in stably hSOS1-reconstituted DT40 cells is measured by a RAC pulldown assay. Low anti-BCR dosage is used for stimulation. Percentages relative to the wild-type maximum activation are shown. Data are representative of two experiments.

activity for both Ras and Rac, in which SOS's atypical Dbl homology/Pleckstrin homology (DH-PH) domain may perform the exchange reaction of GDP for GTP on Rac (53–56). Rac is typically positioned upstream of the MKK3/6-p38 MAPK pathway, although most research has been done in nonlymphoid cell types (33, 40). As an initial start to map a pathway from SOS1 toward p38 in lymphoid cells, we examined activation of the small GTPase Rac. GTP loading of Rac induced by BCR stimulation was drastically reduced in SOS1⁻ SOS2⁻ DT40 cells. RasGRPs are not predicted to have Rac GEF activity (17). Surprisingly, Rac activation was also impaired in RasGRP1⁻ RasGRP3⁻ cells, albeit more modestly (Fig. 7A). The differences in RasGRP and SOS requirements for Rac activation somewhat paralleled their degree of requirement for MKK3/6 and p38 activation but completely contrasted the need for RasGRP or SOS in terms of ERK activation (Fig. 7A); i.e., compared to SOS, RasGRP deficiency results in more-modest Rac and p38 defects but more-severe ERK activation impairment. Supporting a potential SOS-Rac-MKK3/6-p38 pathway, stable reconstitution of SOS1⁻ SOS2⁻ cells with W729E hSOS1 resulted in an effective rescue of BCR-induced Rac activation, mirroring the MKK3/6 and p38 activation rescue, approximating the levels obtained in WT hSOS1-reconstituted cells (Fig. 7B).

Computational explorations of SOS's role in Rac-p38 activation. We built a coarse-grained computational model to formulate new hypotheses that might be explored to provide mechanistic underpinnings to our discovery of SOS's role in Rac-p38 activation and that (unlike ERK activation) the allosteric pocket of SOS is not critical for p38. First, we focused on the differences in activation profiles of Rac and p38 (Fig. 7A): RasGRP1⁻ RasGRP3⁻ cells displayed a significant defect in Rac activation but fairly robust p38 activation; in contrast, SOS1⁻ SOS2⁻ cells had even lower Rac activation and failed to activate p38 effectively. We considered two possible mechanisms to explain this: (i) Rac activated by RasGRP-mediated pathways may be localized in a different compartment than that activated by SOS-mediated pathways, and SOS-activated Rac is more efficient in activating p38 (this is not our focus here but may be tested in future imaging studies), and (ii) a threshold amount of active Rac might be needed to

effectively activate p38, and RasGRP1⁻ RasGRP3⁻ cells can generate enough active Rac to cross that threshold but SOS1⁻ SOS2⁻ cells cannot. To test the second hypothesis, we introduced a thresholding effect for Rac-p38 activation. In biochemical systems, this is most conveniently modeled by using a Hill coefficient greater than 1, as this result is in a nonlinear dependence. We determined that a Hill coefficient of 2 for p38 activation would be sufficient to produce the thresholding effect observed in Fig. 7A.

Next, we investigated whether SOS may function as a RacGEF, an adaptor, or both. Published work indicated that SOS may possess RacGEF activity through its DH-PH domain (53) and/or functions as an adaptor affecting LAT oligomerization which may help recruit and stabilize RacGEFs at the LAT signalosome (57). In our coarse-grained computational model, we assumed that RasGRP also facilitates the stable formation of the LAT signalosome by a cooperative mechanism (12) and hence may regulate RacGEFs as well. We then predicted the Rac-p38 activation profiles for wild-type, RasGRP-deficient, and SOS-deficient cells and SOS cells with disrupted RacGEF activity (DH-PH^mut) under three scenarios (Fig. 8): SOS is both a RacGEF and an adaptor, SOS is only an adaptor, and SOS is only a RacGEF. For panels A and D, DH-PH^mut leaves SOS's adaptor functionality intact, and hence, the Rac activation profile for DH-PH^mut falls between that for the wild type and that for SOS deficiency, crossing the threshold to fully activate P38. For panels B and E, DH-PH^mut does not alter SOS's adapter function and has the same Rac-p38 activation profile as the wild type; for panels C and F, DH-PH^mut completely impairs SOS's RasGEF functions and the DH-PH mutant is as deleterious as SOS deficiency. These simulations suggest that the observed Rac and p38 activation patterns may be a result of either SOS's RacGEF or adaptor function or a combination of the two, which we experimentally tested next.

BCR-induced p38 activation does not require enzymatic activities of SOS1. To test computer-based predictions, we sought to cripple SOS1's enzymatic functions in a manner that would keep a potential adapter function intact. We have previously demonstrated that an F929A substitution in SOS1 abrogates RasGEF activity (Fig. S26 in reference 10). SOS contains a DH-PH domain that potentially may function as a Rac GEF in addition to a Ras
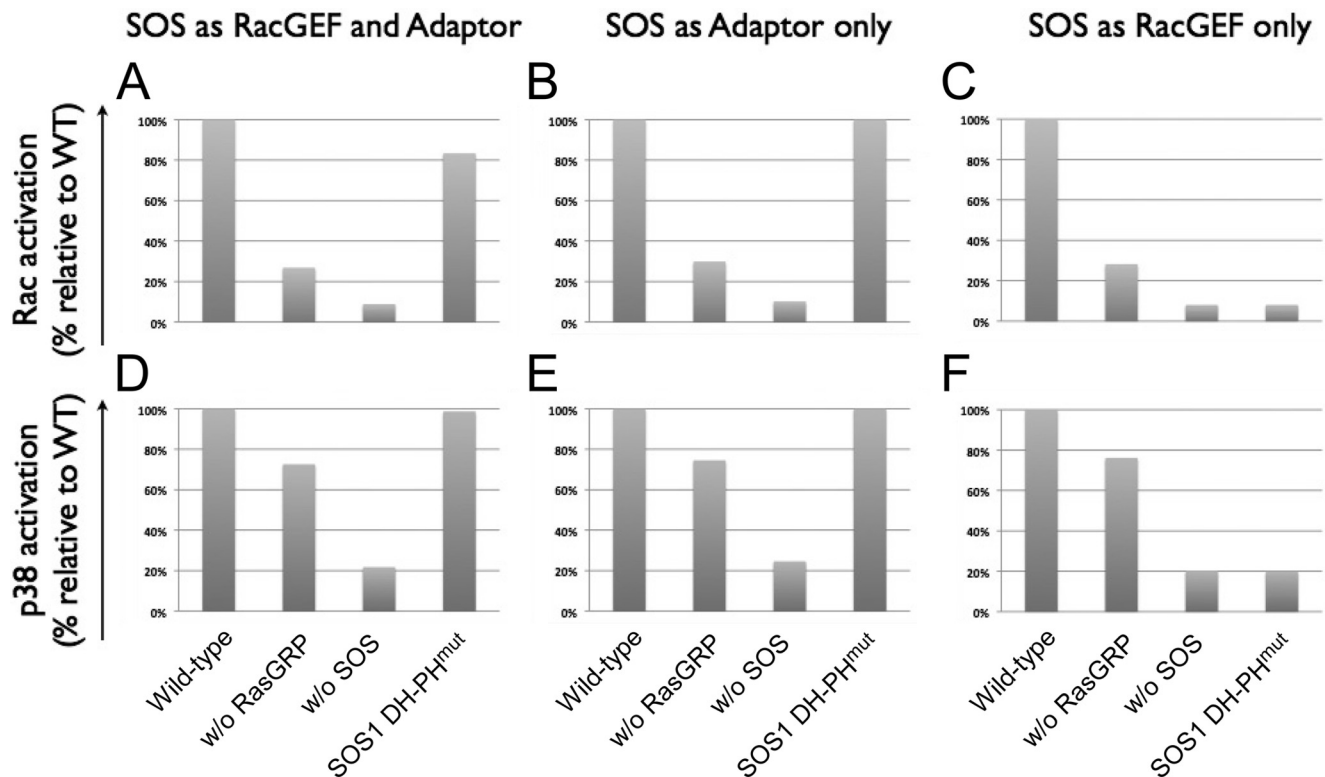
FIG 8 Computational predictions for SOS activating the Rac-p38 pathway. When SOS functions as both a RacGEF and an adaptor (A and D), an adaptor only (B and E), and a RacGEF only (C and F), the activation profile of Rac-p38 for cells with the DH-PH domain mutant SOS is between that for wild-type SOS and that for SOS1$^-$ SOS2$^-$ (A and D), the same as that for wild-type SOS (B and E), and the same as that for SOS1$^-$ SOS2$^-$ (C and F).

GEF (53). No evidence for direct GTP loading of Rac by SOS is available. Instead, a distinct SOS1 complex in association with EPS8 and E3b1/Abi-1 cofactors was shown to have *in vitro* RacGEF activity (55). SOS1's DH domain is atypical (58), making it challenging to design function-impairing point mutations. However, composite deletions in the Dbl oncogene resulted in reduced *in vitro* activation of the small GTPase Cdc42 (59) and inspired studies with a similarly mutated DH domain of SOS1 in fibroblast focal transformation assays (38). A similar 7-amino-acid mutation in the Rac exchange factor Vav (LLLQELV to IIIQ DAA) results in severely impaired TCR-induced Rac activation in Jurkat T cells (60).

We first generated SOS1-DBL^{mut}, an expression construct of human SOS1 with the LHYFELL-to-IIIRDII substitution (38). Repeated attempts to stably reconstitute SOS1$^-$ SOS2$^-$ DT40 cells with SOS1 F929A and SOS1 DBL^{mut} were unsuccessful (data not shown). We therefore resorted to a transient-transfection approach. To this end, we first developed an intracellular FACS approach for p38 phosphorylation (Fig. 9A) so that p38 activation could be assessed without purifying and manipulating transfected cells prior to stimulation and analysis. Next, we transfected SOS1$^-$ SOS2$^-$ DT40 cells with WT, F929A, or DBL^{mut} hSOS1 cells, stimulated these with anti-BCR antibodies, and performed simultaneous intracellular FACS stainings for phospho-p38 and hSOS1. Comparisons of cells expressing equal amounts of SOS1 via the electronic gating strategy depicted in Fig. 9B demonstrated that SOS1 F929A and SOS1 DBL^{mut} restored BCR-induced p38 activation in SOS1$^-$ SOS2$^-$ DT40 cells with a similar efficiency as WT

SOS1 (Fig. 9E and F). Even a lower level of BCR stimulation did not reveal significant defects in p38 activation in cells reconstituted with SOS1-DBL^{mut} (data not shown). In contrast, the same perturbations in the RasGEF and DH domains of SOS1 did impact the magnitude of BCR-induced ERK activation (Fig. 9C and D). Thus, SOS1 appears to play an adapter role in the pathway that leads to p38 activation, whereas allosteric regulation of its catalytic function is critical for ERK activation (Fig. 10).

DISCUSSION

In the present study, we combined computer simulations and biological experiments in cell lines and primary cells to interrogate the requirements for antigen receptor-induced activation of the ERK and p38 MAPK pathways. We find that sensitive and bimodal ERK activation occurs in thymocytes and cell lines (Fig. 1). Bimodal ERK activation critically relies on allosteric activation of SOS1, and an allosteric pocket W729E mutant SOS1 signals to ERK in an analog manner (Fig. 3). In agreement with initial facilitation of allosteric activation of SOS by RasGRP1-derived RasGTP, pharmacological or genetic perturbations of the PLCγ-RasGRP1-Ras pathway in thymocytes and cell lines drastically impair the ERK output (Fig. 5). In contrast to ERK, antigen receptor-induced phosphorylation of p38 is modest and depends on SOS more than on RasGRP but is not affected by mutation of its allosteric pocket in cell lines (Fig. 5 and 6). Moreover, p38 activation does not appear to be affected by crippling mutations in either SOS1's RasGEF domain or its DH domain, which argues that SOS1 functions as an adapter in the p38 pathway (Fig. 8 and 9).
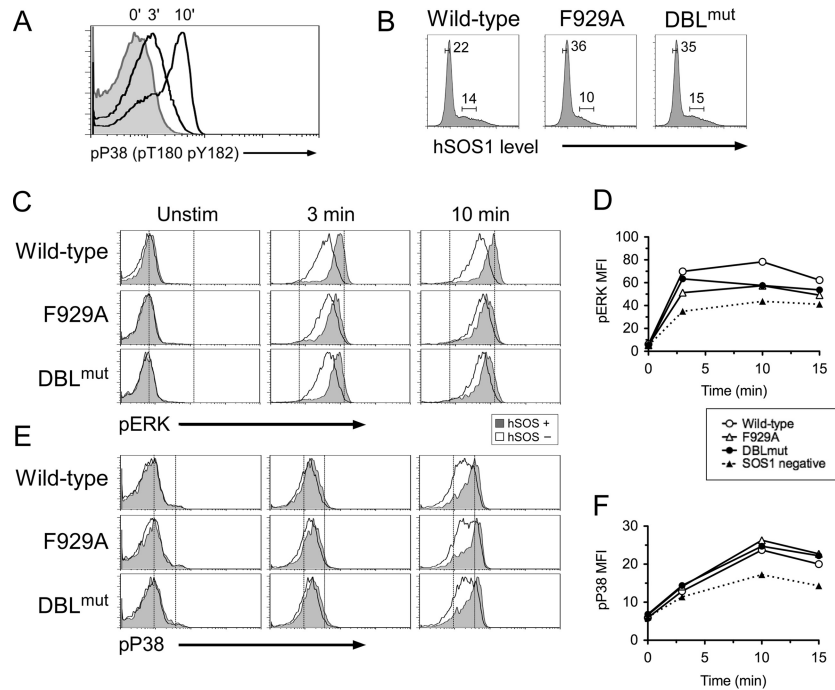
FIG 9 Enzymatic activity of SOS1 is dispensable for BCR-induced p38 activation. (A) Flow cytometric assay of phospho-p38 induced by BCR cross-linking in wild-type DT40 cells. (B) hSOS1 expression profile of transiently transfected SOS1/2 DT40 cells. Two gates show hSOS1-positive (hSOS+) and -negative (hSOS−) populations. (C and E) BCR-induced ERK and p38 activation in transiently transfected SOS1/2 DT40 cells. The hSOS1− subset (open histogram) of each transfection is compared with the hSOS1+ subset (gray histogram) as gated in panel B. (C) Two arbitrarily chosen reference lines in the histogram plot represent basal (left) and maximal (right) pERK intensities of wild-type hSOS1 transfection. (E) Reference line represents basal pP38 intensity. (D and F) Graphical representation of pERK and phospho-p38 mean fluorescence intensities (MFI) shown in panels C and E. "SOS1 negative" represents the average phospho-p38 MFI value of the hSOS− subset in three samples. Data are representative of two experiments.

These findings provide mechanistic insights into the differential activation of ERK and p38 MAPK, which are proposed to play opposing roles during thymocyte selection (13, 26). SOS also plays a critical role downstream of the EGF receptor and other receptor tyrosine kinases (21, 22), and allosteric activation of SOS plays a critical role in EGF-stimulated Ras activation (39). Therefore, our results and hypotheses not only provide new insights into thymocyte MAPK selection signals but also provide a framework for future studies on the impact of distinct MAPK pathway activation in other cellular systems.

Pharmacological inhibition of p38 blocks *in vitro* negative selection of thymocytes (32), but a clear understanding of TCR-induced p38 activation is lacking to date (49). Here we focused on a potential role for the small GTPase Rac, since studies in nonlymphoid cells have positioned Rac upstream of the MKK3/6-p38 MAPK pathway (33, 40) and also postulated that SOS may contain RacGEF activity (54–56). We find that BCR-induced Rac activation is severely impaired in SOS1⁻ SOS2⁻ DT40 cells but is efficiently rescued by reconstitution with both WT and allosteric pocket mutant SOS1, paralleling the requirements of SOS for p38 activation (Fig. 3). In support of this pathway, inhibition of RacGTP accumulation correlates with impaired BCR-induced p38 activity in DT40 cells (61). RasGRP also contributes to RacGTP generation, albeit more modestly than SOS, but does not appear to contribute much to p38 activation (Fig. 5 and 7).

In T cells but not in B cells, it has been reported that antigen receptor stimulation can directly link to p38 activation via lck-ZAP70 activation, via an alternative pathway that bypasses conventional MAPK cascade components, such as LAT and MKK3/6 (49). We explored the LAT-independent pathway but were not able to reproduce the normal p38 activation that had been reported in the LAT-deficient J.CaM2 cell line (50). Instead, we find a defect in p38 activation in J.CaM2 cells (Fig. 5C). It is, however, difficult to rule out the existence of an alternative p38 pathway in J.CaM2 cells because these cells express reduced levels of surface TCR (62), which leads to downstream impairments, such as the suppressed TCR-induced ZAP70 activation in J.Cam2 cells (Fig. 5C), and the alternative pathway is known to be dependent on ZAP70. It is worth noting that blocking DAG production completely abolished TCR-induced MKK3/6 activation, while downstream p38 activation is only partially impaired in U73122-treated Jurkat cells (Fig. 5B). The phospho-p38 reduction is especially more pronounced at the later time point. The residual p38 activation in the near absence of phospho-MKK3/6 might come from an alternative p38 activation pathway (Fig. 5A and B). We postulate that TCR-induced p38 activation may be the sum of two temporally separated pathways: an alternative pathway mediating the early time point, while the later p38 activation is through a conventional MKK3/6-dependent p38 activation pathway. In addition, it is very possible that there are temporal or qualitative differences in mono- and dual phosphorylation. These hypotheses, as well as the differences between p38 activation in T cells and B cells that appear to lack the alternative pathway, are important areas for future research, requiring careful analyses of pT180-p38 and pT180/Y182-p38 following different stimuli, ideally also in-
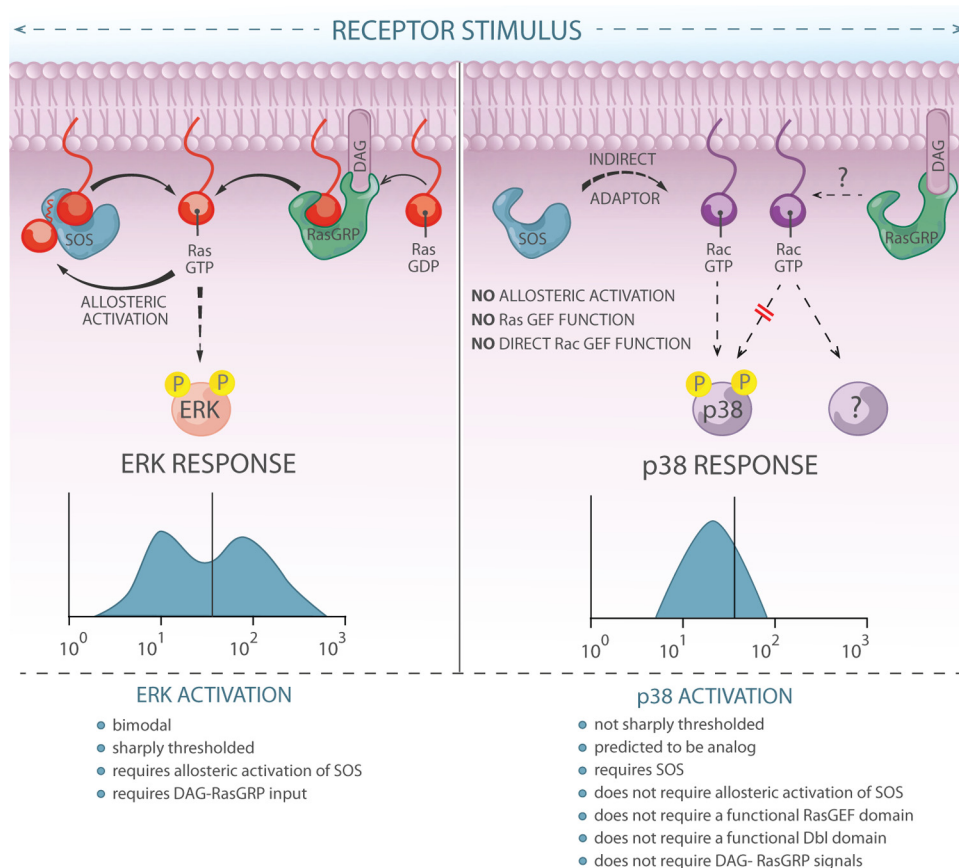
FIG 10 Graphic representation of the contrasting roles of SOS in activating the ERK pathway versus the p38 pathway. ERK activation is bimodal and sharply thresholded. These characteristics critically rely on allosteric activation of SOS. In contrast, p38 activation is not sharply thresholded. Whereas optimal p38 activation does require the presence of SOS1, it does not depend on allosteric activation of SOS1, on an intact RasGEF domain, or on an intact DH domain. These results suggest that SOS1 has an adaptor function in the p38 pathway. Graphic design by Anna Hupalowska.

cluding the mouse models, such as the recently generated p38 knock-in mice (63).

Since the allosteric pocket of SOS is not involved in Rac activation, the defect in Rac activation in RasGRP-deficient cells cannot be explained by impaired allosteric activation of SOS acting as a RacGEF. Instead, we postulate that RasGRP-dependent Rac activation involves a different RacGEF and may couple to downstream pathways other than p38 activation. How RasGRP contributes to Rac activation, what RacGEF is involved, and at what cellular localization Rac activation occurs are important problems for future research. Potential candidates include Tiam1 and Vav (64, 65). Whereas Tiam1 has not been connected to antigen receptor stimulation (66), its RacGEF activity is stimulated by binding to RasGTP (67) and may therefore be RasGRP dependent. Vav family proteins are the best-studied RacGEFs downstream of lymphocyte antigen receptor (68). Vav is not directly responsive to RasGTP, but Vav's GEF activity is regulated indirectly by RasGTP, coupling to its effector phosphatidylinositol 3-kinase (65, 69). Additionally, several studies indicate cross talk between Vav and RasGRP1 (70–72).

Exactly through what mechanism SOS1 functions as an adapter in a Rac-p38 pathway in lymphocytes remains to be resolved through future studies. Complexes of Grb2 and SOS1 at a 2:1 ratio were shown to mediate clustering of multiple LATs and

associated proteins in T cells (57, 73), and it is feasible that the function of RacGEFs like Vav is impacted by LAT clustering. Conversely, Vav has recently been reported to stabilize T cell microclusters that contain the adaptors LAT and SLP76 (74); thus, lymphocyte Rac-p38 activation is likely impacted by many factors.

We anticipate that our studies here will stimulate future investigations of SOS and its role in lymphocyte MAPK activation and thymocyte selection. We hypothesize that strong TCR signal input, as would occur in thymocytes that carry potentially self-reactive TCR and need to be deleted, results in digital ERK activation that depends on allosteric activation of SOS. However, given the data with ERK1 and ERK2 doubly deficient (30) and SOS1 and SOS2 doubly deficient (31) thymocytes, we postulate that the digital ERK activation may be merely a passenger effect of the strong TCR signal and not a driver of negative selection. As such, SOS-dependent strong digital ERK activation, while important for mature T cell activation, may be irrelevant for negative selection. It may also be a mechanism to rapidly downregulate ERK activation by strongly engaging negative feedback loops, and not having sustained ERK activation may be required for negative selection. It has to be noted that some residual bimodal ERK activation was detected in SOS1 and SOS2 doubly deficient thymocytes whereas deficiency for only SOS1 does appear to result in a loss of distinct bimodal ERK activation patterns (31). One possible explanation

for this phenomenon is that complete deficiency for both SOS1 and SOS2 likely results in increased access to Grb2 for other proteins, such as Themis1. Themis1 is a relatively recently identified protein that is expressed predominantly in thymocytes and not in B cells, interacts with Grb2, and positively regulates ERK activation (75–77). We have also described digital ERK activation patterns for TCR-stimulated peripheral T cells in the past (10). Recently, SOS1 has been suggested to be of more limited importance in TCR-induced ERK activation in peripheral T cells (78), although FACS patterns of ERK activation were not examined in this study. Future studies should address the question of whether differences in SOS-mediated ERK activation with the various experimental models are a reflection of compensatory mechanisms or due to the developmental stage of the cell population in the analysis.

We hypothesize that strong TCR input leading to relatively modest p38 activation helps drive negative selection and propose that SOS plays an important role here whereas RasGRP's contribution is more minor. However, Rasgrp1's contribution toward p38 may become more critical when SOS function is limiting, which is supported by a recent study demonstrating compensatory mechanisms between RasGRP1 and SOS1 during negative selection of thymocytes (31). Given the many functions that SOS may fulfill and our results that point to an adaptor function for SOS1 in Rac and p38 activation and a feedback-regulated catalytic function for ERK activation, we anticipate that future studies of specific point mutant versions of SOS will be most informative and will reveal unanticipated compensation mechanisms.

ACKNOWLEDGMENTS

REFERENCES

1. **Chang L, Karin M.** 2001. Mammalian MAP kinase signalling cascades. Nature **410**:37–40.
2. **Marshall CJ.** 1995. Specificity of receptor tyrosine kinase signaling: transient versus sustained extracellular signal-regulated kinase activation. Cell **80**:179–185.
3. **Santos SD, Verveer PJ, Bastiaens PI.** 2007. Growth factor-induced MAPK network topology shapes Erk response determining PC-12 cell fate. Nat. Cell Biol. **9**:324–330.
4. **Ferrell JE, Jr, Machleder EM.** 1998. The biochemical basis of an all-or-none cell fate switch in Xenopus oocytes. Science **280**:895–898.
5. **Markevich NI, Hoek JB, Kholodenko BN.** 2004. Signaling switches and bistability arising from multisite phosphorylation in protein kinase cascades. J. Cell Biol. **164**:353–359.
6. **O'Shaughnessy EC, Palani S, Collins JJ, Sarkar CA.** 2011. Tunable signal processing in synthetic MAP kinase cascades. Cell **144**:119–131.
7. **Tian T, Harding A, Inder K, Plowman S, Parton RG, Hancock JF.** 2007. Plasma membrane nanoswitches generate high-fidelity Ras signal transduction. Nat. Cell Biol. **9**:905–914.
8. **Altan-Bonnet G, Germain RN.** 2005. Modeling T cell antigen discrimination based on feedback control of digital ERK responses. PLoS Biol. **3**:e356. doi:10.1371/journal.pbio.0030356.
9. **Harding A, Tian T, Westbury E, Frische E, Hancock JF.** 2005. Subcellular localization determines MAP kinase signal output. Curr. Biol. **15**:869–873.
10. **Das J, Ho M, Zikherman J, Govern C, Yang M, Weiss A, Chakraborty AK, Roose JP.** 2009. Digital signaling and hysteresis characterize ras activation in lymphoid cells. Cell **136**:337–351.
11. **Lin J, Harding A, Giurisato E, Shaw AS.** 2009. KSR1 modulates the sensitivity of mitogen-activated protein kinase pathway activation in T cells without altering fundamental system outputs. Mol. Cell. Biol. **29**:2082–2091.
12. **Prasad A, Zikherman J, Das J, Roose JP, Weiss A, Chakraborty AK.** 2009. Origin of the sharp boundary that discriminates positive and negative selection of thymocytes. Proc. Natl. Acad. Sci. U. S. A. **106**:528–533.
13. **Starr TK, Jameson SC, Hogquist KA.** 2003. Positive and negative selection of T cells. Annu. Rev. Immunol. **21**:139–176.
14. **Genot E, Cantrell DA.** 2000. Ras regulation and function in lymphocytes. Curr. Opin. Immunol. **12**:289–294.
15. **D'Ambrosio D, Cantrell DA, Frati L, Santoni A, Testi R.** 1994. Involvement of p21ras activation in T cell CD69 expression. Eur. J. Immunol. **24**:616–620.
16. **Swan KA, Alberola-Ila J, Gross JA, Appleby MW, Forbush KA, Thomas JF, Perlmutter RM.** 1995. Involvement of p21ras distinguishes positive and negative selection in thymocytes. EMBO J. **14**:276–285.
17. **Stone JC.** 2011. Regulation and function of the RasGRP family of Ras activators in blood cells. Genes Cancer **2**:320–334.
18. **Dower NA, Stang SL, Bottorff DA, Ebinu JO, Dickie P, Ostergaard HL, Stone JC.** 2000. RasGRP is essential for mouse thymocyte differentiation and TCR signaling. Nat. Immunol. **1**:317–321.
19. **Oh-hora M, Johmura S, Hashimoto A, Hikida M, Kurosaki T.** 2003. Requirement for Ras guanine nucleotide releasing protein 3 in coupling phospholipase C-gamma2 to Ras in B cell receptor signaling. J. Exp. Med. **198**:1841–1851.
20. **Roose JP, Mollenauer M, Ho M, Kurosaki T, Weiss A.** 2007. Unusual interplay of two types of Ras activators, RasGRP and SOS, establishes sensitive and robust Ras activation in lymphocytes. Mol. Cell. Biol. **27**:2732–2745.
21. **Buday L, Downward J.** 1993. Epidermal growth factor regulates p21ras through the formation of a complex of receptor, Grb2 adapter protein, and Sos nucleotide exchange factor. Cell **73**:611–620.
22. **Lowenstein EJ, Daly RJ, Batzer AG, Li W, Margolis B, Lammers R, Ullrich A, Skolnik EY, Bar-Sagi D, Schlessinger J.** 1992. The SH2 and SH3 domain-containing protein GRB2 links receptor tyrosine kinases to ras signaling. Cell **70**:431–442.
23. **Margarit SM, Sondermann H, Hall BE, Nagar B, Hoelz A, Pirruccello M, Bar-Sagi D, Kuriyan J.** 2003. Structural evidence for feedback activation by Ras·GTP of the Ras-specific nucleotide exchange factor SOS. Cell **112**:685–695.
24. **Freedman TS, Sondermann H, Friedland GD, Kortemme T, Bar-Sagi D, Marqusee S, Kuriyan J.** 2006. A Ras-induced conformational switch in the Ras activator Son of sevenless. Proc. Natl. Acad. Sci. U. S. A. **103**:16692–16697.
25. **Chakraborty AK, Das J, Zikherman J, Yang M, Govern CC, Ho M, Weiss A, Roose J.** 2009. Molecular origin and functional consequences of digital signaling and hysteresis during Ras activation in lymphocytes. Sci. Signal. **2**:pt2. doi:10.1126/scisignal.266pt2.
26. **Palmer E.** 2003. Negative selection—clearing out the bad apples from the T-cell repertoire. Nat. Rev. Immunol. **3**:383–391.
27. **Fischer AM, Katayama CD, Pages G, Pouyssegur J, Hedrick SM.** 2005. The role of erk1 and erk2 in multiple stages of T cell development. Immunity **23**:431–443.
28. **Gong Q, Cheng AM, Akk AM, Alberola-Ila J, Gong G, Pawson T, Chan AC.** 2001. Disruption of T cell signaling networks and development by Grb2 haploid insufficiency. Nat. Immunol. **2**:29–36.
29. **Kortum RL, Sommers CL, Alexander CP, Pinski JM, Li W, Grinberg A, Lee J, Love PE, Samelson LE.** 2011. Targeted Sos1 deletion reveals its critical role in early T-cell development. Proc. Natl. Acad. Sci. U. S. A. **108**:12407–12412.
30. **McGargill MA, Ch'en IL, Katayama CD, Pages G, Pouyssegur J, Hedrick SM.** 2009. Cutting edge: extracellular signal-related kinase is not required for negative selection of developing T cells. J. Immunol. **183**:4838–4842.
31. **Kortum RL, Sommers CL, Pinski JM, Alexander CP, Merrill RK, Li W, Love PE, Samelson LE.** 2012. Deconstructing Ras signaling in the thymus. Mol. Cell. Biol. **32**:2748–2759.
32. **Sugawara T, Moriguchi T, Nishida E, Takahama Y.** 1998. Differential roles of ERK and p38 MAP kinase pathways in positive and negative selection of T lymphocytes. Immunity **9**:565–574.
33. **Rincon M, Pedraza-Alva G.** 2003. JNK and p38 MAP kinases in CD4+ and CD8+ T cells. Immunol. Rev. **192**:131–142.

34. **Werlen G, Hausmann B, Naeher D, Palmer E.** 2003. Signaling life and death in the thymus: timing is everything. Science **299:**1859–1863.

35. **Riese MJ, Grewal J, Das J, Zou T, Patil V, Chakraborty AK, Koretzky GA.** 2011. Decreased diacylglycerol metabolism enhances ERK activation and augments CD8+ T cell functional responses. J. Biol. Chem. **286:**5254–5265.

36. **Locasale JW, Shaw AS, Chakraborty AK.** 2007. Scaffold proteins confer diverse regulatory properties to protein kinase cascades. Proc. Natl. Acad. Sci. U. S. A. **104:**13307–13312.

37. **Gillespie DT.** 1977. Exact stochastic simulation of coupled chemical reactions. J. Phys. Chem. **81:**2340–2361.

38. **Qian X, Vass WC, Papageorge AG, Anborgh PH, Lowy DR.** 1998. N terminus of Sos1 Ras exchange factor: critical roles for the Dbl and pleckstrin homology domains. Mol. Cell. Biol. **18:**771–778.

39. **Boykevisch S, Zhao C, Sondermann H, Philippidou P, Halegoua S, Kuriyan J, Bar-Sagi D.** 2006. Regulation of ras signaling dynamics by Sos-mediated positive feedback. Curr. Biol. **16:**2173–2179.

40. **Dong C, Davis RJ, Flavell RA.** 2002. MAP kinases in the immune response. Annu. Rev. Immunol. **20:**55–72.

41. **Ebinu JO, Stang SL, Teixeira C, Bottorff DA, Hooton J, Blumberg PM, Barry M, Bleakley RC, Ostergaard HL, Stone JC.** 2000. RasGRP links T-cell receptor signaling to Ras. Blood **95:**3199–3203.

42. **Waters SB, Holt KH, Ross SE, Syu LJ, Guan KL, Saltiel AR, Koretzky GA, Pessin JE.** 1995. Desensitization of Ras activation by a feedback disassociation of the SOS-Grb2 complex. J. Biol. Chem. **270:**20883–20886.

43. **Porfiri E, McCormick F.** 1996. Regulation of epidermal growth factor receptor signaling by phosphorylation of the ras exchange factor hSOS1. J. Biol. Chem. **271:**5871–5877.

44. **Corbalan-Garcia S, Yang SS, Degenhardt KR, Bar-Sagi D.** 1996. Identification of the mitogen-activated protein kinase phosphorylation sites on human Sos1 that regulate interaction with Grb2. Mol. Cell. Biol. **16:**5674–5682.

45. **Zhao H, Li YY, Fucini RV, Ross SE, Pessin JE, Koretzky GA.** 1997. T cell receptor-induced phosphorylation of Sos requires activity of CD45, Lck, and protein kinase C, but not ERK. J. Biol. Chem. **272:**21625–21634.

46. **Kamioka Y, Yasuda S, Fujita Y, Aoki K, Matsuda M.** 2010. Multiple decisive phosphorylation sites for the negative feedback regulation of SOS1 via ERK. J. Biol. Chem. **285:**33540–33548.

47. **Bhalla US, Ram PT, Iyengar R.** 2002. MAP kinase phosphatase as a locus of flexibility in a mitogen-activated protein kinase signaling network. Science **297:**1018–1023.

48. **Sondermann H, Soisson SM, Boykevisch S, Yang SS, Bar-Sagi D, Kuriyan J.** 2004. Structural analysis of autoinhibition in the Ras activator Son of sevenless. Cell **119:**393–405.

49. **Ashwell JD.** 2006. The many paths to p38 mitogen-activated protein kinase activation in the immune system. Nat. Rev. Immunol. **6:**532–540.

50. **Salvador JM, Mittelstadt PR, Guszczynski T, Copeland TD, Yamaguchi H, Appella E, Fornace AJ, Jr, Ashwell JD.** 2005. Alternative p38 activation pathway mediated by T cell receptor-proximal tyrosine kinases. Nat. Immunol. **6:**390–395.

51. **Mittelstadt PR, Yamaguchi H, Appella E, Ashwell JD.** 2009. T cell receptor-mediated activation of p38{alpha} by mono-phosphorylation of the activation loop results in altered substrate specificity. J. Biol. Chem. **284:**15469–15474.

52. **Roose JP, Diehn M, Tomlinson MG, Lin J, Alizadeh AA, Botstein D, Brown PO, Weiss A.** 2003. T cell receptor-independent basal signaling via Erk and Abl kinases suppresses RAG gene expression. PLoS Biol. **1:**e53. doi:10.1371/journal.pbio.0000053.

53. **Nimnual A, Bar-Sagi D.** 2002. The two hats of SOS. Sci. STKE **2002:**pe36. doi:10.1126/stke.2002.145.pe36.

54. **Nimnual AS, Yatsula BA, Bar-Sagi D.** 1998. Coupling of Ras and Rac guanosine triphosphatases through the Ras exchanger Sos. Science **279:**560–563.

55. **Scita G, Nordstrom J, Carbone R, Tenca P, Giardina G, Gutkind S, Bjarnegard M, Betsholtz C, Di Fiore PP.** 1999. EPS8 and E3B1 transduce signals from Ras to Rac. Nature **401:**290–293.

56. **Mettouchi A, Klein S, Guo W, Lopez-Lago M, Lemichez E, Westwick JK, Giancotti FG.** 2001. Integrin-specific activation of Rac controls progression through the G(1) phase of the cell cycle. Mol. Cell **8:**115–127.

57. **Houtman JC, Yamaguchi H, Barda-Saad M, Braiman A, Bowden B, Appella E, Schuck P, Samelson LE.** 2006. Oligomerization of signaling complexes by the multipoint binding of GRB2 to both LAT and SOS1. Nat. Struct. Mol. Biol. **13:**798–805.

58. **Soisson SM, Nimnual AS, Uy M, Bar-Sagi D, Kuriyan J.** 1998. Crystal structure of the Dbl and pleckstrin homology domains from the human Son of sevenless protein. Cell **95:**259–268.

59. **Hart MJ, Eva A, Zangrilli D, Aaronson SA, Evans T, Cerione RA, Zheng Y.** 1994. Cellular transformation and guanine nucleotide exchange activity are catalyzed by a common domain on the dbl oncogene product. J. Biol. Chem. **269:**62–65.

60. **Kuhne MR, Ku G, Weiss A.** 2000. A guanine nucleotide exchange factor-independent function of Vav1 in transcriptional activation. J. Biol. Chem. **275:**2185–2190.

61. **Hashimoto A, Okada H, Jiang A, Kurosaki M, Greenberg S, Clark EA, Kurosaki T.** 1998. Involvement of guanosine triphosphatases and phospholipase C-gamma2 in extracellular signal-regulated kinase, c-Jun NH2-terminal kinase, and p38 mitogen-activated protein kinase activation by the B cell antigen receptor. J. Exp. Med. **188:**1287–1295.

62. **Markegard E, Trager E, Yang CW, Zhang W, Weiss A, Roose JP.** 2011. Basal LAT-diacylglycerol-RasGRP1 signals in T cells maintain TCRα gene expression. PLoS One **6:**e25540. doi:10.1371/journal.pone.0025540.

63. **Jirmanova L, Sarma DN, Jankovic D, Mittelstadt PR, Ashwell JD.** 2009. Genetic disruption of p38α Tyr323 phosphorylation prevents T-cell receptor-mediated p38α activation and impairs interferon-gamma production. Blood **113:**2229–2237.

64. **Tybulewicz VL, Henderson RB.** 2009. Rho family GTPases and their regulators in lymphocytes. Nat. Rev. Immunol. **9:**630–644.

65. **Welch HC, Coadwell WJ, Stephens LR, Hawkins PT.** 2003. Phosphoinositide 3-kinase-dependent activation of Rac. FEBS Lett. **546:**93–97.

66. **Gerard A, van der Kammen RA, Janssen H, Ellenbroek SI, Collard JG.** 2009. The Rac activator Tiam1 controls efficient T-cell trafficking and route of transendothelial migration. Blood **113:**6138–6147.

67. **Lambert JM, Lambert QT, Reuther GW, Malliri A, Siderovski DP, Sondek J, Collard JG, Der CJ.** 2002. Tiam1 mediates Ras activation of Rac by a PI(3)K-independent mechanism. Nat. Cell Biol. **4:**621–625.

68. **Turner M, Billadeau DD.** 2002. VAV proteins as signal integrators for multi-subunit immune-recognition receptors. Nat. Rev. Immunol. **2:**476–486.

69. **Han J, Luby-Phelps K, Das B, Shu X, Xia Y, Mosteller RD, Krishna UM, Falck JR, White MA, Broek D.** 1998. Role of substrates and products of PI 3-kinase in regulating activation of Rac-related guanosine trisphosphates by Vav. Science **279:**558–560.

70. **Caloca MJ, Zugaza JL, Matallanas D, Crespo P, Bustelo XR.** 2003. Vav mediates Ras stimulation by direct activation of the GDP/GTP exchange factor Ras GRP1. EMBO J. **22:**3326–3336.

71. **Reynolds LF, de Bettignies C, Norton T, Beeser A, Chernoff J, Tybulewicz VL.** 2004. Vav1 transduces T cell receptor signals to the activation of the Ras/ERK pathway via LAT, Sos, and RasGRP1. J. Biol. Chem. **279:**18239–18246.

72. **Zugaza JL, Caloca MJ, Bustelo XR.** 2004. Inverted signaling hierarchy between RAS and RAC in T-lymphocytes. Oncogene **23:**5823–5833.

73. **Sherman E, Barr V, Manley S, Patterson G, Balagopalan L, Akpan I, Regan CK, Merrill RK, Sommers CL, Lippincott-Schwartz J, Samelson LE.** 2011. Functional nanoscale organization of signaling molecules downstream of the T cell antigen receptor. Immunity **35:**705–720.

74. **Sylvain NR, Nguyen K, Bunnell SC.** 2011. Vav1-mediated scaffolding interactions stabilize SLP-76 microclusters and contribute to antigen-dependent T cell responses. Sci. Signal. **4:**ra14. doi:10.1126/scisignal.2001178.

75. **Fu G, Vallee S, Rybakin V, McGuire MV, Ampudia J, Brockmeyer C, Salek M, Fallen PR, Hoerter JA, Munshi A, Huang YH, Hu J, Fox HS, Sauer K, Acuto O, Gascoigne NR.** 2009. Themis controls thymocyte selection through regulation of T cell antigen receptor-mediated signaling. Nat. Immunol. **10:**848–856.

76. **Johnson AL, Aravind L, Shulzhenko N, Morgun A, Choi SY, Crockford TL, Lambe T, Domaschenz H, Kucharska EM, Zheng L, Vinuesa CG, Lenardo MJ, Goodnow CC, Cornall RJ, Schwartz RH.** 2009. Themis is a member of a new metazoan gene family and is required for the completion of thymocyte positive selection. Nat. Immunol. **10:**831–839.

77. **Lesourne R, Uehara S, Lee J, Song KD, Li L, Pinkhasov J, Zhang Y, Weng NP, Wildt KF, Wang L, Bosselut R, Love PE.** 2009. Themis, a T cell-specific protein important for late thymocyte development. Nat. Immunol. **10:**840–847.

78. **Warnecke N, Poltorak M, Kowtharapu BS, Arndt B, Stone JC, Schraven B, Simeoni L.** 2012. TCR-mediated Erk activation does not depend on Sos and Grb2 in peripheral human T cells. EMBO Rep. **13:**386–391.